

Constructing different ‘bridges’ for interfacial electron transfer in azobenzene LB/SAM composite bilayers

H.Z. Yu¹, N. Xia, J. Zhang, Z.F. Liu*

Center for Intelligent Materials Research (CIMR), College of Chemistry and Molecular Engineering, Peking University, Beijing 100871, China

Received 22 October 1997; received in revised form 8 December 1997

Abstract

Two methods, Langmuir–Blodgett (LB) and self-assembly (SA), were used in the present work to fabricate certain interfacial structures for the study of long-range electron transfer. We have successfully constructed two different ‘bridges’ for the interfacial electron transfer in azobenzene LB/SAM composite bilayer systems. One has ionic bonding character, while the other has face-to-face hydrogen bonding at the interface of an ABD (4-octyl-4’-(3-carboxy-trimethylene-oxy)-azobenzene) LB monolayer and the underlying aminothiols SAM. These structures have been confirmed by using RA-FTIR and contact angle titration. Furthermore, the apparent electron transfer rate across the ionic bonding ‘bridge’ is much more rapid than in the hydrogen-bonded case, indicating that the interfacial structure plays a crucial role in the long-range electron transfer kinetics. © 1998 Elsevier Science S.A. All rights reserved.

Keywords: Electron transfer; Azobenzene; Self-assembled monolayers; Langmuir–Blodgett films; Interfacial design

1. Introduction

Two methods, Langmuir–Blodgett (LB) and self-assembly (SA), perhaps the most convenient and useful ways for preparing molecularly tailored interfaces with controlled spatial and geometric constraints [1], were used in our work to fabricate certain interfacial structures for the study of long-distance interfacial electron transfer. One issue of particular interest is the clarification of electron transfer behavior at various interfaces in biological systems [2,3]. Combining both the SA and LB techniques, two different mechanisms for long-range electron transfer, ‘through-bond tunneling’ and ‘through-space tunneling’ have been investigated by McLendon’s group [4,5]. We present herein another comparative study, which could help us to understand

the role of different interaction forces, ionic and hydrogen bonding, in the process of long-range electron transfer.

The electrochemically active species involved in our system is azobenzene, which has a relatively complex redox mechanism [6]. In previous studies, we extensively investigated its structural properties and electrochemical behavior in both LB films and SAMs [7–9], which provided significant knowledge for the present work.

2. Experimental

4-Octyl-4’-(3-carboxy-trimethylene-oxy)-azobenzene (referred to as ABD) was purchased from Dojindo Laboratory (Kumamoto, Japan). 2-Aminoethanethiol (2-AET) and 4-aminothiophenol (4-ATP) were obtained from Tokyo Kasei (TCl, Tokyo). All the chemicals were of reagent grade and used without further purification.

* Corresponding author. Fax: +86 10 62757157; e-mail: lzf@chemms.chem.pku.edu.cn

¹ Present address: Arthur Amos Noyes Laboratories, Division of Chemistry and Chemical Engineering, California Institute of Technology, Pasadena, CA 91125, USA.

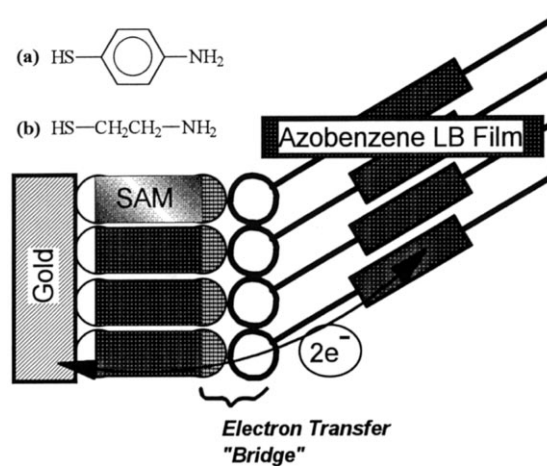
The preparation of aminothiols SAMs on gold and the further deposition of ABD LB monolayers followed a similar procedure as described in detail in our previous paper [9]. Gold substrates were prepared by vacuum deposition (10^{-4} Pa at 0.1 nm s^{-1}) of high-purity gold (99.99%) onto glass slides that had been precoated with chromium to improve adhesion (10 nm of Cr followed by 150–200 nm Au). Before use in experiments, the gold substrate was first cleaned with 'piranha solution' (7:3 concentrated $\text{H}_2\text{SO}_4/30\%\text{H}_2\text{O}_2$. **Caution:** 'piranha solution' reacts violently with many organic materials and should be handled with great care.) at 90° for 5–10 min, and rinsed exhaustively with distilled, deionized water and absolute ethanol. The gold substrate was subsequently immersed in an 1.0 mM alkanethiol + ethanol solution for about 24 h. The alkanethiol-modified electrodes were checked for quality and uniformity by means of contact angle titration and spectroscopic measurements [10]. Langmuir–Blodgett transfer of ABD monolayers to the alkanethiol-modified electrode was done by spreading and compressing 0.1 mmol/l ABD + CHCl_3 solution on a subphase surface, and finally vertically dipping the SAM covered gold substrate into the subphase at 0.1 cm min^{-1} .

Electrochemical experiments were carried out in a three-electrode cell. An $\text{Ag}|\text{AgCl}|\text{satd KCl}$ and a Pt wire were used as the reference and counter electrodes, respectively. The cis isomer of ABD was produced by 2 min UV (350 nm) irradiation of the trans-form ABD film. The electrolyte solution was 0.1 mol/l NaClO_4 that was buffered using the Britton–Robinson method.

Infrared spectra were obtained with a Perkin-Elmer System 2000 FT-IR spectrometer equipped with a MCT detector. A SPECAC variable-angle reflection attachment was used for reflection absorption measurements and at an incidence angle of 82° (near grazing angle). Contact angle experiments were performed with a contact angle goniometer (Model JJC-2, The Fifth Optical Instrument Factory of Changchun) under ambient conditions (18–20°C, 50–60% relative humidity) using yellow light to illuminate the water droplet.

3. Results and discussion

The two bilayer systems built up are modeled here in Scheme 1; an ABD LB monolayer was transferred onto a 2-AET and a 4-APT SAM on a gold substrate, respectively. At first glance, the difference between the two systems (a) and (b) is trivial, as the $-\text{CH}_2\text{CH}_2-$ is simply replaced by the electrophilic $-\text{Ph}-$ group, which is believed to accelerate the electron transfer. However, given more consideration, it is this nuance that perhaps could result in two totally different interfacial electron transfer behaviors.



Scheme 1. Configuration of the azobenzene LB/SAM composite bilayer systems.

In order to obtain the necessary experimental evidence for a better understanding of the above interfacial structures, contact angle titration was employed as a convenient method for studying the SAMs' surface properties. The static contact angles on a 4-APT SAM are shown in Fig. 1 as a function of pH value. Each point represents an average of at least four measurements. The so-called contact angle titration curve has two clear-cut plateaus with a transitional region at pH 6–8. It has the same feature, but with a different turning point as that of the 2-AET SAMs we previously reported [11]. The pH value of the turning point in the titration curve corresponds to the $\text{pK}_{1/2}$ for the acid/base equilibrium in the SAM (the pH value at which half of the acidic/basic end groups in a SAM transform into their conjugate base/acid). We can thus determine the $\text{pK}_{1/2}$ of the 2-AET SAM and the 4-APT SAM to be 12.2 ± 0.2 and 7.3 ± 0.2 , respectively. The $\text{pK}_{1/2}$ value is in good accordance with that obtained by means of measuring differential interfacial capacitance

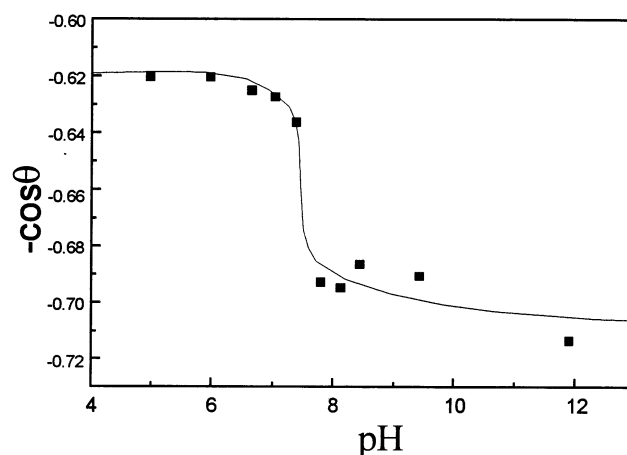
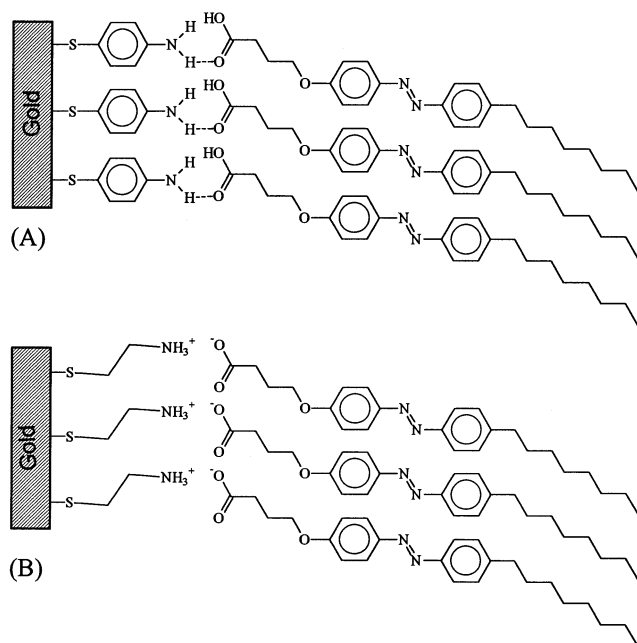


Fig. 1. Contact angle titration curve of a 4-APT SAM modified gold surface.



Scheme 2. The proposed interfacial structure for the azobenzene LB/SAM composite bilayer: (a) ABD-LB/4-ATP SAM; (b) ABD-LB/2-AET SAM.

[12]. All these values are significantly larger than those of bulk-phase data, which can be explained by the effect of the surface charge state as well as localized pH environments at the surface [10,13]. This is similar to the frequently observed increase of surface $pK_{1/2}$ values for acid group terminated monolayers [14]. Nevertheless, the different $pK_{1/2}$ values enable us to know the different charge states of these monolayers, that is, the amino groups in the surface of the 2-AET SAM exist as an ionic state when the pH value is less than 12.2. The 4-APT monolayer will change from an ionic state ($-\text{NH}_3^+$) to $-\text{NH}_2$ when the pH value becomes greater than 7.3. The basicity of the two amino compounds freely dispersed in solution can be easily compared, and the considerable electron-conjugating ability of the benzyl group causes 4-APT to be the weaker base. Our measurements of contact angles demonstrate that, in a two-dimensional and well-organized environment, the above relation is still in effect.

To complete the construction of the systems, as shown in Scheme 1, the 2-AET SAM and the 4-APT SAM modified gold electrodes were used as substrates for transferring an LB monolayer of ABD molecules. On the basis of contact angle titration results, we can infer that, after being vertically immersed into the subphase, the 2-AET monolayer is undoubtedly in its ionic form (NH_3^+). However, the 4-APT SAM, which has a $pK_{1/2}$ of 7.3, is likely to exist in the $-\text{NH}_2$ state. Therefore, the final two SAM/LB combined systems should possess different interfacial structures as shown in Scheme 2. The ionic bonding ($-\text{NH}_3^+ - \text{OOC}-$) and

van der Waals interaction (hydrogen bonding probably results from the nature of $-\text{NH}_2$ and $-\text{COOH}$ groups) are the predominate interfacial forces in the ABD-LB/4-APT SAM and the ABD-LB/2-AET SAM bilayer systems, respectively.

We then resorted to IR spectra for some decisive proofs for the structures, especially the interfacial configurations in Scheme 2. In Fig. 2(a,b), the IR spectra of a 2-AET SAM and a 4-APT SAM are presented in the range of $800-3500 \text{ cm}^{-1}$. The benzene ring stretches at 1592 and 1492 cm^{-1} , combined with the N-H stretch at 3361 cm^{-1} , demonstrate the formation of a 4-APT monolayer on a gold surface. Similarly, the existence of a 2-AET monolayer is evidenced by the bands at 3360 cm^{-1} for N-H stretching and 1100 cm^{-1} for C-N stretching. Fig. 2(c) and Fig. 2(d) show the RA-FTIR spectra for an ABD-LB/2-AET SAM and an ABD-LB/4-APT SAM, respectively. The presence of an ABD monolayer is clearly evidenced by the series of characteristic vibration bands shown in the spectra. For instance, in the case of the ABD-LB/2-AET SAM (see Fig. 2c), the bands at 1592 and 1501 cm^{-1} are due to the in-plane vibration of the benzene ring; the bands at 1253 , 1153 and 847 cm^{-1} are attributed to the $\phi\text{-O}$ stretching, $\phi\text{-N}$ stretching and out-of-plane bending of $\phi\text{-H}$, respectively. In the higher frequency region, the C-H stretching vibration bands are also observed clearly. The peaks at 2966 and 2958 cm^{-1} can be assigned to the CH_3 asymmetric in-plane stretching mode and the asymmetric out-of-plane stretching mode, and the bands at 2927 and 2854 cm^{-1} to the CH_2 asymmetric and symmetric modes, respectively. Our previous report showed that the absorptions of alkanethiol SAMs with very short chain lengths were very weak [9]. The strong peaks in the present study should be attributed mainly to the C-H vibration of ABD molecules rather than the 2-AET molecules. The most important result of our FTIR data is the ability now to ascertain the interfacial structures of the azobenzene LB/SAM bilayer systems by comparing the spectra taken before (Fig. 2(a,b)) and after the LB film deposition (Fig. 2(c,d)). In the case of the ABD-LB/4-APT SAM, the absorption band for N-H stretching in the 4-APT SAM at 3361 cm^{-1} (Fig. 2(a)) can still be found in the bilayer system (Fig. 2(c) at 3369 cm^{-1}). Furthermore, there is an intense band attributed to the $-\text{C}=\text{O}$ stretch at 1721 cm^{-1} , indicating that the head group of the ABD molecules is probably in the form of $-\text{COOH}$ and might form face-to-face hydrogen bonding with the surface $-\text{NH}_2$ group of the 4-APT SAM. Taken together, it is reasonable to conclude that the amino group at the surface of the SAM is in the form of $-\text{NH}_2$, and that the head group of the ABD LB film has not dissociated. That is to say, the formation of the ABD-LB/4-APT SAM bilayer system is based only on a kind of weak interaction like face-to-face hydrogen

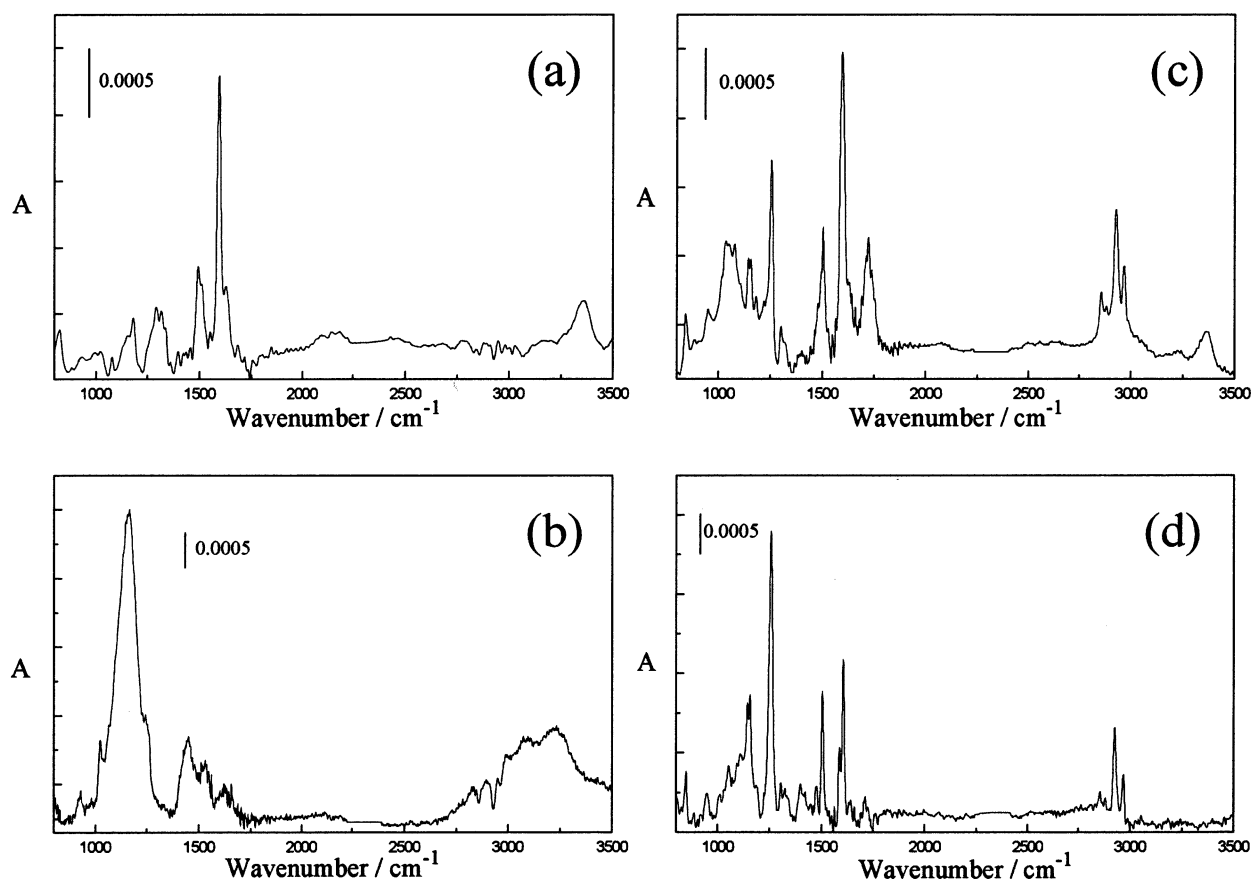


Fig. 2. RA-FTIR spectra of azobenzene LB/SAM composite bilayers: (a) 4-ATP SAM on Au; (b) 2-AET SAM on Au; (c) ABD-LB/4-ATP SAM bilayer; (d) ABD-LB/2-AET SAM bilayer.

bonding (Scheme 2a). For the comparative ABD-LB/2-AET SAM system, the spectra changes are quite different from what we have described above. The N–H vibrational band in the 2-AET SAM (Fig. 2(b), at 3360 cm^{-1}) diminished after the LB film transfer (Fig. 2(d)). A new band at 1397 cm^{-1} , representative of the vibrational mode of $-\text{COO}^-$ appeared in Fig. 2(d), and there is no corresponding band for $-\text{C}=\text{O}$ stretching as was seen in Fig. 2(b). The asymmetric stretching band for $-\text{COO}^-$ does not appear due to the selection rule of reflectance IR spectroscopy. These spectra characteristics indicate that both the amino groups at the surface of the SAM and the head groups of the LB monolayer are in their ionic states. It is expected that the ionic interaction takes control of the ‘bridge’ between the ABD LB film and the underlying 2-AET SAM.

Thus, Scheme 2 is confirmed by both contact angle titration and RA-FTIR measurements, providing a prototypical system for electrochemical studies on different interfacial structures and heterogeneous electron transfer kinetic behavior.

Cyclic voltammetric measurements were performed in the usual way. Fig. 3 shows the cyclic voltammogram (CV) of an ABD-LB/4-ATP SAM bilayer system, ob-

tained after 2 min of UV irradiation. Two coupled redox waves with a considerably large peak-to-peak separation were observed clearly. The waves were very stable and excellently reproducible within several tens of experimental runs. The observed electrochemical re-

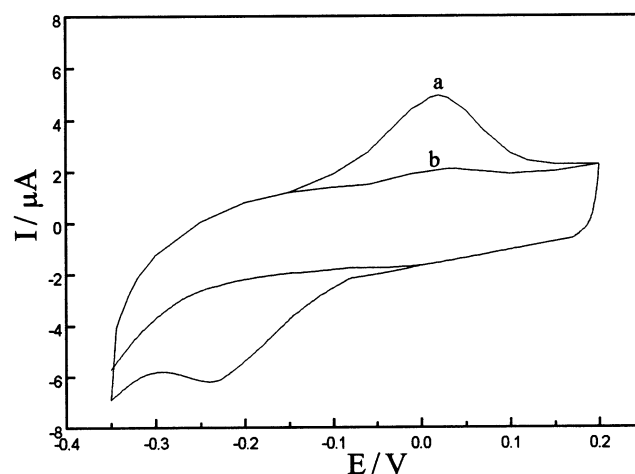


Fig. 3. Cyclic voltammetric responses of an ABD-LB/4-ATP SAM bilayer. (a) After 2 min UV irradiation of the film. (b) In the dark. Scan rate, 200 mV s^{-1} ; pH 6.3.

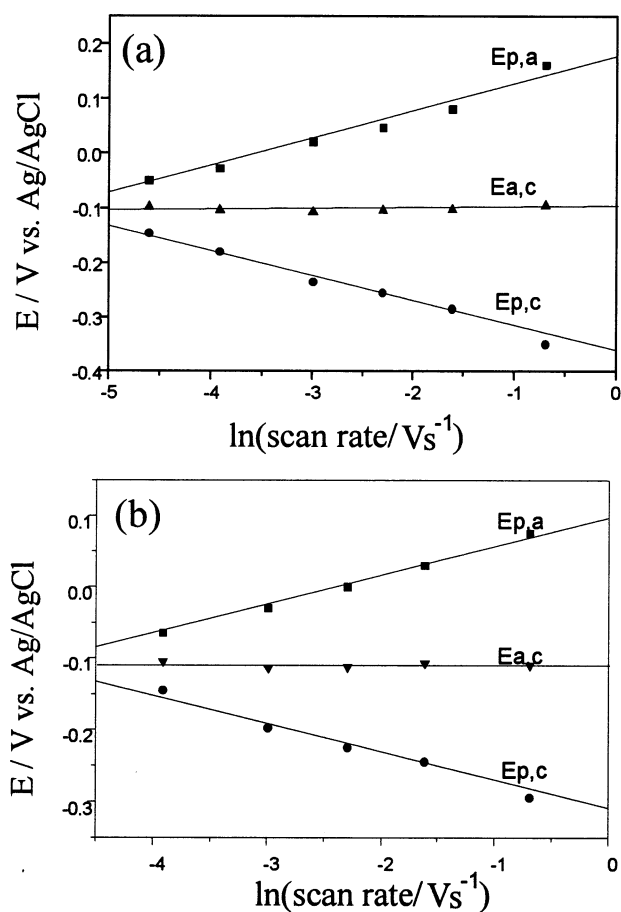


Fig. 4. Linear dependences of anodic peak potential $E_{p,a}$ (■), cathodic peak potential $E_{p,c}$ (●), and midpoint potential $E_{a,c}$ (▲) ($E_{a,c} = (E_{p,a} + E_{p,c})/2$) on the logarithmic scan rate. (a) ABD-LB/4-ATP SAM bilayer; (b) ABD-LB/2-AET SAM bilayer.

sponses were attributed to the reduction and re-oxidation of the immobilized *cis*-form azobenzene group [7,9]. These observations indicate that our specially constructed ‘bridge’ is stable and allows electron transport across it. We already have reported a similar electrochemical behavior of the ABD-LB/2-AET SAM system in a previous paper [9]. A linear relationship between scan rate and peak current was found in all cases, confirming that the current is due to the redox reaction of the azobenzene immobilized in the bilayer on the Au electrode. The separation between the anodic and cathodic peak increased with the potential scan rate, indicating that the electrode reaction was controlled by electron transfer kinetics.

Fig. 4 shows the scan rate dependence of the cathodic and anodic peak potentials for the azobenzene LB/SAM bilayer systems. The plot clearly indicates that the cathodic and anodic peak potentials change linearly with the logarithmic scan rate. According to Laviron’s treatment [15], the standard heterogeneous rate constant of electron transfer may be obtained in a straight-

forward manner from Eq. (1) and Eq. (2) under totally irreversible conditions,

$$E_{p,c} = E^{\circ} - (RT/\alpha nF) \ln(\alpha nFv/RTk_{app}) \quad (1)$$

$$E_{p,a} = E^{\circ} + [RT/(1-\alpha)nF] \ln[(1-\alpha)nFv/RTk_{app}] \quad (2)$$

where α is the transfer coefficient and v is the potential scan rate. Assuming that E° and the product αn are independent of the sweep rate, the graphs of $E_{p,c} \sim \ln(v)$ and $E_{p,a} \sim \ln(v)$ have been fitted with linear regression lines, as shown in Fig. 4. Their slopes are $RT/\alpha nF$ and $RT/(1-\alpha)nF$, respectively. Thus, the values of αn and $(1-\alpha)n$ were obtained and substituted back into Eq. (1) and Eq. (2) to solve for k_{app} .

According to the above procedure, the rate constants for the ABD-LB/4-ATP SAM and the ABD-LB/2-AET SAM systems at pH 6.3 were calculated to be 0.09 and 0.18 s^{-1} , respectively. The present results are in good accordance with those previously reported [9]. They are smaller than those obtained for simple adsorption of unsubstituted azobenzenes on electrode surfaces [6], but much larger than that of *trans*-azobenzene in a highly organized self-assembled monolayer [8,16,17]. The difference in electron transfer rates for these three kinds of systems is believed to reflect the correlation between the molecular packing and the redox behavior of azobenzene in organized monolayer assemblies [8,9,16,17].

However, at present, we are more interested in two points. First, both ionic-bonded and hydrogen-bonded interfaces serve as efficient ‘bridges’ for the long-range electron transfer in these organized molecular assemblies. Second, there is a two-fold difference of electron transfer rates between the two azobenzene LB/SAM bilayer systems. Such a deviation is significantly larger than the probable experimental errors (which have an upper range of 10%) in evaluating the electron transfer rate constants. Therefore, the difference probably originates from the structural nature of these bilayer systems. Although the microscopic mechanism for such a unique phenomenon is probably rather complex and is unclear at our current research stage, we believe that the difference could be attributed partially to the different electron traveling ‘bridges’ in these systems. In other words, comparison of the k_{app} might reflect properly the influences of the two kinds of interfacial structures, ionic bonding and hydrogen bonding, on the respective electron transfer behavior. McLendon and his colleagues have found that in a ferrocene LB/SAM bilayer that has a non-bonded interfacial structure, the electron transfer rate is almost 2 orders of magnitude lower than that for the analogous ferrocene chemically bound to Au through alkanethiols of similar bond length [5]. They attribute the higher rate in the latter to a through-bond mechanism, whereas in the former there exists a single ‘break’ in the chemical bond network cutting off the through-bond passway. This sug-

gestion is valuable for us here to describe the difference between electron transfer through the ionic bonding 'bridge' and the hydrogen-bonding narrow 'bridge'. Whereas the latter might be taken as a 'throat' for through-bond tunneling long-range electron transfer of azobenzene to the electrode surface, the former may serve as a broad 'bridge' for the through-bond electron tunneling. Moreover, in consideration of the benzyl group in the 4-ATP SAM which should increase the value of k_{app} , it is reasonable to believe that the real relative efficiency of ionic bonding on electron transfer rates is more than twice than that of hydrogen bonding.

Therien and co-workers recently figured out a direct comparison of photoinduced electron transfer rates through hydrogen, σ and π bonds by using a zinc(II) and iron(III) system [18]. They have shown that the electron transfer rate through a hydrogen-bonded interface is even greater than that provided by an analogous interface composed entirely of carbon-carbon σ bonds. Both our present results and their findings have shown the potential of hydrogen-bonded interfaces in long-range electron transfer, but the direct comparison of these two different systems is not at hand because of the different experimental methods and interfacial configuration. Another problem with the present approach we should address here is the effect of possible different packing structures of the two SAMs. As we already know, the molecular packing and organization in the SAMs are dependent on the molecular nature, such as geometrical and dynamic properties. From our experiments, both 4-ATP and 2-AET molecules form uniform and reproducible monolayers on the gold surface, and there is no direct evidence to describe the significant difference in the packing structures of these two monolayer systems [10]. Nevertheless, the results to date shed light on the fact that interfacial structural details add a very important contribution to the long-range electron transfer behavior. The detailed evaluation of the interfacial structure by systematically changing the pH values and constructing well-defined interfaces, as well as further theoretical investigations are presently underway.

4. Conclusion

The combined experimental investigations by both contact angle titration and RA-FTIR measurement indicated that different interfacial structures are built in the azobenzene LB/SAM composite bilayer systems. There is an ionic interaction between the head group of

the ABD LB monolayer and the dissociated amino group of the 2-AET SAM on gold, while there is only hydrogen bonding in the ABD-LB/4-ATP SAM system. The electron transfer rates in the two systems are different, probably due to the varied interfacial structures, a 'bridge' effect versus a 'throat' for the through-bond tunneling electron transfer. The present results demonstrate that the detailed nature of the 'bridge' plays an important role in long-distance electron transfer, which should have implications on the electron transfer studies of biological systems.

Acknowledgements

Financial support from the State Committee of Science and Technology, the State Educational Committee and National Natural Science Foundation of China are gratefully acknowledged. H.Z. Yu would like to thank Dr. G. Kloster at Caltech for his critical review and comments on the manuscript.

References

- [1] A. Ulman, *From Langmuir-Blodgett to Self-Assembly, An Introduction to Ultrathin Organic Films*, Academic Press, Boston, MA, 1991.
- [2] G. McLendon, *Acc. Chem. Res.* 21 (1988) 160.
- [3] J.N. Onuchic, D.N. Beratan, J.R. Winkler, H.B. Gray, *Annu. Rev. Biophys. Biomol. Struct.* 21 (1992) 349.
- [4] L.H. Guo, J.S. Facci, G. McLendon, *J. Phys. Chem.* 99 (1995) 4106.
- [5] L.H. Guo, J.S. Facci, G. McLendon, *J. Phys. Chem.* 99 (1995) 8458.
- [6] E. Laviron, Y. Mugnier, *J. Electroanal. Chem.* 111 (1980) 337.
- [7] Z.F. Liu, K. Hashimoto, A. Fujishima, *J. Electroanal. Chem.* 324 (1992) 259.
- [8] H.Z. Yu, Y.Q. Wang, J.Z. Cheng, J.W. Zhao, S.M. Cai, H. Inokuchi, A. Fujishima, Z.F. Liu, *Langmuir* 12 (1996) 2843.
- [9] Z.F. Liu, C.X. Zhao, M. Tang, S.M. Cai, *J. Phys. Chem.* 100 (1996) 17377.
- [10] H.Z. Yu, N. Xia, H.X. He, Z.F. Liu, manuscript in preparation.
- [11] H.Z. Yu, J.W. Zhao, Y.Q. Wang, S.M. Cai, Z.F. Liu, *J. Electroanal. Chem.* 438 (1997) 221.
- [12] M.A. Bryant, R.M. Crooks, *Langmuir* 9 (1993) 385.
- [13] K.I. Mullen, D.X. Wang, L.G. Crane, K.T. Carron, *Anal. Chem.* 64 (1992) 930.
- [14] S.E. Creager, J. Clarke, *Langmuir* 10 (1994) 3675.
- [15] E. Laviron, *J. Electroanal. Chem.* 101 (1979) 19.
- [16] Y.Q. Wang, H.Z. Yu, J.Z. Cheng, J.W. Zhao, S.M. Cai, Z.F. Liu, *Langmuir* 12 (1996) 5466.
- [17] H.Z. Yu, H.B. Shao, Y. Luo, H.L. Zhang, Z.F. Liu, *Langmuir* 13 (1997) 5774.
- [18] P.J.F. De Rege, S.A. Williams, M.J. Therien, *Science* 269 (1995) 1409.